

Chordal Conversion based Convex Iteration Algorithm for Three-phase Optimal Power Flow Problems

Wei Wang, *Student Member, IEEE*, Nanpeng Yu, *Senior Member, IEEE*,

Abstract—The three-phase optimal power flow (OPF) problem has recently attracted a lot of research interests due to the need to coordinate the operations of large-scale and heterogeneous distributed energy resources (DERs) in unbalanced electric power distribution systems. The non-convexity of the three-phase OPF problem is much stronger than that of the single-phase OPF problem. Instead of applying the semidefinite programming relaxation technique, this paper advocates a convex iteration algorithm to solve the non-convex three-phase OPF problem. To make the convex iteration algorithm computationally efficient for large-scale distribution networks, the chordal conversion based technique is embedded in the convex iteration framework. By synergistically combining the convex iteration method and the chordal based conversion technique, the proposed three-phase OPF algorithm is not only computationally efficient but also guarantees global optimality when the trace of the regularization term becomes zero. At last, to further improve the computational performance, a greedy grid partitioning algorithm is proposed to decompose a single large matrix representing a distribution network to many smaller matrices. The simulation results using standard IEEE test feeders show that the proposed algorithm is computationally efficient, scalable, and yields global optimal solutions while resolving the rank conundrum.

Index Terms—Chordal conversion, convex iteration, distribution system operator, three-phase optimal power flow.

NOMENCLATURE

E_k^p, F_k^p	Real part and imaginary part of the voltage at node k with phase p .
e_i	Standard basis vector.
g_{ik}^{pm}, b_{ik}^{pm}	Conductance and susceptance between node i with phase p and node k with phase m in the line admittance matrix.
G_{ik}^{pm}, B_{ik}^{pm}	Conductance and susceptance between node i with phase p and node k with phase m in the admittance matrix.
G	The set of nodes with controllable generations in the power distribution network.
M_k^p	Matrix defined for voltage magnitude calculation for node i with phase p .
N	The set of all nodes in the power network.
N_A	Total number of decomposed areas.
n_s	Number of areas to search for further partitions at the current stage.
$P_{D_k}^p, Q_{D_k}^p$	Fixed real and reactive load at node k with phase p .
$P_{G_k}^p, Q_{G_k}^p$	Fixed real and reactive power generation at node k with phase p .

$P_{k,inj}^p, Q_{k,inj}^p$	Real and reactive power injection at node k with phase p .
$\underline{P}_k^p, \overline{P}_k^p$	Lower and upper limit of real power capacity of controllable distributed generation at node k with phase p .
P_{ik}^{pm}, Q_{ik}^{pm}	Real and reactive power flow from node i with phase p to node k with phase m .
$\underline{Q}_k^p, \overline{Q}_k^p$	Lower and upper limit of reactive power capacity of controllable distributed generation at node k with phase p .
V	Nodal voltage vector.
V_k^p	Voltage at node k with phase p .
$\underline{V}_k^p, \overline{V}_k^p$	Lower and upper limit of voltage magnitude at node k with phase p .
X_l^{ext}	Sub-matrix of X associated with nodes in the l -th extended sub-area.
$X_l^{ext(r)}$	Sub-matrix of X_l^{ext} associated with nodes in the l -th extended sub-area intersected with the r -th extended sub-area.
y_{ik}^{pm}	Line admittance between node i with phase p and node k with phase m .
Y	Admittance matrix.
Y_k^p, \overline{Y}_k^p	Admittance matrices defined for real and reactive power injection calculation.
$Y_{ik}^p, \overline{Y}_{ik}^p$	Admittance matrices defined for real and reactive power flow calculation.
$Y_k^{p(l)}, \overline{Y}_k^{p(l)}$	Admittance matrices defined for real and reactive power injection calculation associated with the branches in the l -th extended area.
$Y_{ik}^{p(l)}, \overline{Y}_{ik}^{p(l)}$	Admittance matrices defined for real and reactive power flow calculation associated with the nodes in the l -th extended area.

I. INTRODUCTION

IN the past 20 years, wholesale power markets operating in transmission systems have been effective at coordinating the operations of thousands of centralized power plants. Recently the growth in volume and diversity of DERs and smart buildings is transforming the operation of power systems and the design of electricity markets. As DERs and smart buildings continue to penetrate the electric power distribution systems, dynamic resource management and optimization on a large-scale system with thousands of DERs becomes difficult. This difficulty can be addressed with a distribution system market

approach where electricity customers can proactively participate in the resource dispatch and price formation processes. The market approach has been advocated by many researchers and policy makers. For example, the New York Public Service Commission kicked off a proposal called Reforming the Energy Vision (REV) which attempts to develop distribution system operators (DSOs) that coordinate and facilitate the planning and operations of various DERs and smart buildings. Leaving aside the policy debates surrounding the DSO markets, the operation of DERs relies on a key algorithm, the three-phase OPF algorithm, which still needs significant development. The discrete control elements including switches and transformer taps also play a very important role in distribution system operations [1]–[4]. However, it is beyond the scope of this paper.

The single-phase OPF problem for the transmission system has been studied extensively in the past 50 years. The transmission system can be treated as a single-phase system in the OPF problem due to the relatively balanced electricity loads across three phases and periodically transposed transmission lines. The single-phase OPF problem is highly non-convex due to the nonlinear relationship between voltage and power injections. This problem can be solved by numerous algorithms including Newton-based methods [5], [6], linear and quadratic programming [7], nonlinear and polynomial programming [8], interior point methods [9], and heuristic optimization methods [10]. However, none of them guarantees a global optimum. To obtain a global optimum, a SDP relaxation method was recently proposed [11]. The method first transforms the OPF problem to a semidefinite programming problem (SDP) where the only non-convex constraint is a rank-one constraint. If the rank-one constraint is dropped, then convex optimization techniques can be used to solve the problem. The global optimality of this convex relaxation method has been proven for single-phase tree-networks [12] and a small group of mesh networks [13] with some small perturbations in the admittance matrix. Nonetheless, a rank-one solution can not always be achieved with the convex relaxation algorithm. The exactness of the convex relaxation has been investigated in [14], [15]. The convex relaxation approach has been leveraged to develop heuristic algorithms that solve rank-constrained optimization problems [16]–[18]. However, the convergence of these algorithms cannot be guaranteed.

Aside from the rank-one conundrum, the centralized SDP algorithm does not scale very well with the size of the problem [19]. Many researchers attempted to develop and implement distributed algorithms to solve the centralized SDP problem. Reference [20] introduced three distributed schemes to solve the single-phase OPF problem: the auxiliary problem principle (APP), the predictor-corrector proximal multiplier method (PCPM), and the alternating direction multiplier method (ADMM). The ADMM has been widely adopted in developing distributed OPF solvers due to its simplicity and convergence properties [19], [21]–[23]. Although decomposing the main problem into multiple sub-instances of smaller-sized problems makes the solver more efficient, the ADMM can be very slow to converge to high accuracy [24]. In decomposing the main problem many researchers have leveraged the chordal based

matrix completion theory through graph partitioning [25]–[32]. The heuristic matrix combination algorithm and the clique amalgamation method were developed to further improve the computational efficiency of single-phase OPF algorithms by searching for better network decomposition schemes [26], [33].

To coordinate the operations of DERs in the electric power distribution systems, we must solve the three-phase OPF problem. The single-phase OPF problem is insufficient for two reasons. First, the electricity loads on three phases are unbalanced in the distribution systems. Second, the distribution feeders are not transposed. Only a few researchers have studied the three-phase OPF problem [23], [34]. A quasi-Newton method based approach was developed after transforming the OPF problem with implicit function theorem in [34]. Authors in [23] developed a distributed semidefinite programming solver for the three-phase OPF problem based on ADMM and the Lagrangian relaxation method. However, neither of the algorithms guarantees convergence or global optimality. Furthermore, these algorithms are not computationally efficient enough to handle realistic distribution feeders with thousands of buildings and customers.

The main goal of this paper is to develop a computationally efficient and scalable three-phase OPF algorithm which is capable of finding global optimal solutions. Specifically, we first revisit the rank conundrum in solving three-phase OPF problems. A counter example of a three-phase network is provided to show that rank-one solution can not be guaranteed with the SDP relaxation method. To find a global optimal solution efficiently, this paper proposes an innovative three-phase OPF algorithm by synergistically combining the convex iteration technique and the chordal based conversion algorithm. We also propose a greedy algorithm to find an appropriate grid partitioning scheme which results in lower computational complexity. Numerical simulations are conducted on the IEEE test feeders to validate the computational efficiency and scalability of the proposed algorithm and the optimality of the solutions. The simulation results show that the proposed algorithm can find feasible and global optimal solutions even when the SDP relaxation method fails. Furthermore, the greedy grid partition algorithm is shown to be effective in finding an appropriate chordal conversion which makes the overall algorithm computationally efficient. Finally, the simulation results from the IEEE 123-bus and 906-bus test feeders demonstrate the scalability of the proposed algorithm.

The remainder of this paper is organized as follows: Section II formulates the three-phase OPF problem in SDP format with voltages in rectangular form. Section III first presents the convex iteration method and the chordal based conversion technique to solve the non-convex optimization problem. It then describes how to synergistically combine these two methods. In addition, a greedy grid partition algorithm is proposed. The numerical study results of the IEEE distribution test feeders are presented in Section IV. The conclusions are stated in Section V.

II. FORMULATION OF THE THREE-PHASE ACOPF

The SDP formulation of single-phase alternating current OPF (ACOPF) problem was derived with voltages in rectangular form [13]. Reference [23] extended the SDP formulation to three-phase ACOPF problem with complex voltages. In this section, we formulate the three-phase ACOPF problem with voltages in the rectangular form.

A. Matrix Definition

For a three-phase n -node distribution network, define the voltage vector as:

$$V \triangleq [E_1^1, E_1^2, E_1^3 \cdots E_n^1, E_n^2, E_n^3, F_1^1, F_1^2, F_1^3 \cdots F_n^1, F_n^2, F_n^3]^T$$

where E_k^p and F_k^p are the real and imaginary parts of complex voltage at node k with phase p .

Define the matrix Ψ_k^p as

$$\Psi_k^p \triangleq e_{3(k-1)+p} e_{3(k-1)+p}^T Y \quad (1)$$

where Y is the admittance matrix of the distribution network [23] and $e_{3(k-1)+p}$ is the standard basis vector with the $[3(k-1)+p]$ -th element being 1, the only non-zero entry.

$$e_{3(k-1)+p} \triangleq [0, 0, 0, \dots, 1, 0, \dots, 0]^T \quad (2)$$

Define the admittance matrices to be used for power injection calculations as:

$$\mathbf{Y}_k^p \triangleq \frac{1}{2} \begin{bmatrix} \text{Re}(\Psi_k^p + \Psi_k^{pT}) & \text{Im}(\Psi_k^{pT} - \Psi_k^p) \\ \text{Im}(\Psi_k^p - \Psi_k^{pT}) & \text{Re}(\Psi_k^p + \Psi_k^{pT}) \end{bmatrix} \quad (3)$$

$$\bar{\mathbf{Y}}_k^p \triangleq -\frac{1}{2} \begin{bmatrix} \text{Im}(\Psi_k^p + y_k^{pT}) & \text{Re}(\Psi_k^p - \Psi_k^{pT}) \\ \text{Re}(\Psi_k^{pT} - y_k^p) & \text{Im}(\Psi_k^p + \Psi_k^{pT}) \end{bmatrix} \quad (4)$$

Then the real and reactive power injection equations can be rewritten as follows:

$$P_{k,in}^p = \text{Tr}\{\mathbf{Y}_k^p V V^T\} \quad (5)$$

$$Q_{k,in}^p = \text{Tr}\{\bar{\mathbf{Y}}_k^p V V^T\} \quad (6)$$

Define the admittance matrices Ψ_{ik}^p , \mathbf{Y}_{ik}^p , and $\bar{\mathbf{Y}}_{ik}^p$ to be used for branch flow calculations as follows:

$$\Psi_{ik}^p \triangleq e_{3(i-1)+p} \sum_{m=1}^3 (e_{3(i-1)+m} \cdot y_{ik}^{pm} - e_{3(k-1)+m} \cdot y_{ik}^{pm})^T$$

$$\mathbf{Y}_{ik}^p \triangleq \frac{1}{2} \begin{bmatrix} \text{Re}(\Psi_{ik}^p + \Psi_{ik}^{pT}) & \text{Im}(\Psi_{ik}^{pT} - \Psi_{ik}^p) \\ \text{Im}(\Psi_{ik}^p - \Psi_{ik}^{pT}) & \text{Re}(\Psi_{ik}^p + \Psi_{ik}^{pT}) \end{bmatrix} \quad (7)$$

$$\bar{\mathbf{Y}}_{ik}^p \triangleq -\frac{1}{2} \begin{bmatrix} \text{Im}(\Psi_{ik}^p + \Psi_{ik}^{pT}) & \text{Re}(\Psi_{ik}^{pT} - \Psi_{ik}^p) \\ \text{Re}(\Psi_{ik}^{pT} - \Psi_{ik}^p) & \text{Im}(\Psi_{ik}^p + \Psi_{ik}^{pT}) \end{bmatrix} \quad (8)$$

where y_{ik}^{pm} is the line admittance between node i with phase p and node k with phase m .

Then the branch power flow connecting node i and node k with phase p can be rewritten as follows:

$$S_{ik}^p = \text{Tr}\{\mathbf{Y}_{ik}^p V V^T\} + j \text{Tr}\{\bar{\mathbf{Y}}_{ik}^p V V^T\} \quad (9)$$

Define matrix M_i^p as:

$$M_k^p \triangleq \begin{bmatrix} e_{3(k-1)+p} e_{3(k-1)+p}^T & 0 \\ 0 & e_{3(k-1)+p} e_{3(k-1)+p}^T \end{bmatrix} \quad (10)$$

Then the square of voltage magnitude can be rewritten as:

$$|V_i^p|^2 = \text{Tr}\{M_k^p V V^T\} \quad (11)$$

B. Three-phase ACOPF Problem

The objective of the three-phase ACOPF problem in a distribution system is to maximize total social welfare, minimize total power purchase cost, or minimize distribution system losses. The three-phase OPF problem can be formulated in $X = V V^T$ with matrices defined in section II.A as follows:

Formulation 1:

$$\min_X C(X) \quad (12)$$

subject to:

$$P_{G_k}^p - P_{D_k}^p = \text{Tr}\{\mathbf{Y}_k^p X\}, \quad k \in N \setminus G \quad (13)$$

$$Q_{G_k}^p - Q_{D_k}^p = \text{Tr}\{\bar{\mathbf{Y}}_k^p X\}, \quad k \in N \setminus G \quad (14)$$

$$\underline{P}_k^p - P_{D_k}^p \leq \text{Tr}\{\mathbf{Y}_k^p X\} \leq \bar{P}_k^p - P_{D_k}^p, \quad k \in G \quad (15)$$

$$\underline{Q}_k^p - Q_{D_k}^p \leq \text{Tr}\{\bar{\mathbf{Y}}_k^p X\} \leq \bar{Q}_k^p - Q_{D_k}^p, \quad k \in G \quad (16)$$

$$\text{Tr}\{\mathbf{Y}_{ik}^p X\}^2 + \text{Tr}\{\bar{\mathbf{Y}}_{ik}^p X\}^2 \leq (S_{ik}^{max})^2, \quad i, k \in N \quad (17)$$

$$(V_k^p)^2 \leq \text{Tr}\{M_k^p X\} \leq (\bar{V}_k^p)^2, \quad k \in N \quad (18)$$

$$X = V V^T \quad (19)$$

Equation (19) is equivalent to the following two equations:

$$X \succeq 0 \quad (20)$$

$$\text{rank}(X) = 1 \quad (21)$$

In this paper, the objective function (12) is chosen to minimize the total power purchase cost.

$$C(X) = \sum_{p=1}^3 \sum_{k \in G} c_k^p P_k^p \quad (22)$$

where c_k^p and P_k^p are the supply offer price and generation quantity at controllable generation node k with phase p . Equations (13) and (14) enforce real and reactive power balance constraints for load buses. Equations (15) and (16) represent real and reactive power generation capacity constraints for buses with distributed generations. Power flow constraints are modeled in equation (17). Voltage constraint is enforced in equation (18). Equation (19) can be replaced by a positive semidefinite constraint and a rank constraint. The rank constraint is a non-convex constraint.

III. CONVEX ITERATION AND CONVERSION METHOD

A. Rank-one Conundrum Revisited

The rank constraint makes it difficult to solve the reformulated OPF problem. Many researchers tried to solve the OPF problem by applying the semidefinite relaxation technique in which the rank constraint is dropped [11], [13], [15], [23], [27], [33]. Some heuristic methods were developed to recover a rank-one solution for single-phase networks when the semidefinite relaxation technique fails [16], [17]. The existence of global optimal rank-one solution has been proved for single-phase radial network in [12]. It is claimed in [23] that semidefinite relaxation is “exact” for the three-phase OPF problem in a radial network. However, no rigorous proof was provided. The semidefinite relaxation technique did result in global optimal solution in the numerical tests [23]. However, the results are obtained when the supply offer prices of the three phases are exactly the same. In practice, it is not realistic to assume that the supply offer prices from distributed energy resources on three phases will be the same [35]. A counter example is given in this subsection to prove that semidefinite relaxation is not “exact” for three-phase OPF problems.

In order to prove the “exactness” of SDP relaxation for OPF problems of single-phase tree-networks, the geometry of the feasible power injection region is analyzed [12]. Similarly, the feasible power injection region of a three-phase two-node network is studied here. It can be assumed that a network consists of two three-phase nodes connected by a typical distribution line. Define P_1^1, P_1^2, P_1^3 and P_2^1, P_2^2, P_2^3 as the power injections of the three phases at node 1 and node 2 respectively. Assuming the voltage magnitudes are around 1 per unit, the power injections can be calculated with the differences in voltage angles.

The 2-bus three-phase network is analyzed under two scenarios. In the first scenario, it is assumed that the supply offer prices of DERs are the same for all three phases. Then, the OPF problem is equivalent to optimize over the feasible injection region of power summed over three phases. The feasible region on the plane of power injection at node 1 versus node 2, i.e., P_1 versus P_2 , is depicted in Figure 1.

In the second scenario, it is assumed that the supply offer prices are different on the three phases. In this case, the above-mentioned equivalence is no longer valid. The projection of the six-dimensional feasible power injection region onto P_1^1 versus P_2^1 plane for the second scenario is depicted in Figure 2.

In the first scenario, the supply offer prices of the three different phases are the same. Therefore, the feasible power injection region on the P_1 and P_2 plane is approximately an ellipsoid as shown in Figure 1. By dropping the rank constraint, the new feasible region can be obtained by taking the convex hull of the original region, which is the same ellipsoid. The optimal solution is located on the Pareto front of the feasible power injection region. Therefore, relaxing the rank constraint doesn’t influence the optimal solution as the Pareto front of the two feasible power injection regions are the same.

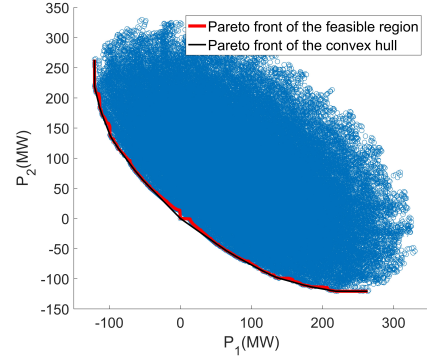


Fig. 1. Feasible power injection region of a two-node network with the same supply offer prices on three phases

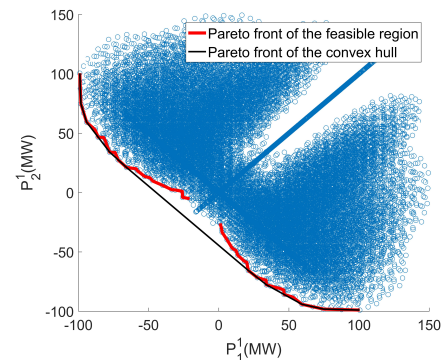


Fig. 2. Feasible power injection region of a two-node network with different supply offer prices on three phases

In the second scenario, the supply offer prices of DERs on three phases are different. The projection of the feasible power injection region onto the P_1^1 and P_2^1 plane is non-convex as shown in Figure 2. Taking convex hull will enlarge the original feasible region. Therefore, the Pareto front of the relaxed problem is different and the solutions with semidefinite relaxation technique will have higher ranks. To resolve the rank conundrum, we advocate the adoption of the convex iteration technique to solve the three-phase OPF problem.

B. Convex Iteration

Instead of directly dropping the rank constraint in Formulation 1, we advocate the adoption of the convex iteration technique to express the rank-constrained optimization problem as iteration of the convex problem sequence (23) and (24) [36] in Formulation 2:

Formulation 2:

$$\min_X C(X) + w \text{Tr}(XW^*)$$

subject to

$$\begin{aligned} X &\in B \\ X &\succeq 0 \end{aligned} \quad (23)$$

$$\min_{W \in S^N} \text{Tr}(X^*W)$$

subject to

$$\begin{aligned} 0 \preceq W \preceq I \\ \text{Tr}(W) = N_X - 1 \end{aligned} \quad (24)$$

where B denotes the feasible region of X defined by equations (13) – (18), W^* represents the optimal solution to semidefinite program (24), and X^* denotes the optimal solution to semidefinite program (23). The size of X and W are both $N_X \times N_X$. The closed-form solution of the second convex optimization problem (24) is

$$W = U(:, 2 : N_X)U(:, 2 : N_X)^T \quad (25)$$

where U can be obtained from the eigenvalue decomposition

$$X^* = U\Lambda U^T \quad (26)$$

The result achieved from SDP relaxation can be used as a starting point, as the convex hull usually provides a tight lower bound. The initial value of the direction matrix can be chosen as the zero matrix.

It has been proved that the convex iteration algorithm always converges and the global optimality can be achieved when the objective function of the second step in the iteration vanishes [36]. In other words, a global optimal solution can be obtained if the convex iteration algorithm converges and the linear regularization term $\text{Tr}(X^*W)$ becomes zero. The optimal direction matrix W_{opt}^* is defined as any positive semidefinite matrix yielding optimal solution X^* of rank one. Therefore, the following two problems are equivalent when W_{opt}^* is found.

$$\begin{aligned} \min \quad & C(X) + w \text{Tr}(XW_{opt}^*) \\ \text{s.t.} \quad & X \in B \\ & X \succeq 0 \end{aligned} \quad \equiv \quad \begin{aligned} \min \quad & C(X) \\ \text{s.t.} \quad & X \in B \\ & X \succeq 0 \\ & \text{rank}(X) = 1 \end{aligned}$$

It should be noted that the convex iteration algorithm is different from the relaxation of the rank-constrained optimization problem. However, at global optimality, the convex iteration formulation is equivalent to the relaxed problem. The convex iteration algorithm was successfully applied in other applications including sensor-network localization and compressed sensing [36]. By contrast, penalization methods [17], [18] tries to recover a rank-one solution from the lower bound of the optimal solution by minimizing either the voltage difference or reactive power loss. The recovered rank-one solution is only near-optimal or local-optimal.

C. Intuition of Convex Iteration Algorithm

The derivation of the convex iteration algorithm can be intuitively explained as follows. For a rank-one positive semidefinite matrix, the largest eigenvalue is also the only non-zero eigenvalue, i.e.,

$$\text{Tr}(X) = \sum_i \lambda(X)_i = \lambda_{max}(X) \quad (27)$$

The rank-one constraint is equivalent to the following constraint:

$$\text{Tr}(X) - \lambda_{max}(X) = 0 \quad (28)$$

where the largest eigenvalue can be obtain by:

$$\max_{\|u\|_2=1} u^T X u$$

Therefore, constraint (28) can be rewritten as:

$$\left\{ \min_{\|u\|_2=1} \text{Tr}(X(I - uu^T)) \right\} = 0$$

This is equivalent to:

$$\left\{ \min_{I \succeq W \succeq 0} \text{Tr}(XW) \right\} = 0 \quad (29)$$

By multiplying the equality constraint (29) with w and adding it to the objective function (12), the original problem in Formulation 1 can be rewritten as:

$$\min_{X, W} C(X) + w \text{Tr}(XW)$$

subject to

$$\begin{aligned} X \in B \\ X \succeq 0 \\ I \succeq W \succeq 0 \end{aligned} \quad (30)$$

As shown in the above optimization problem formulation, the rank-one constraint is re-expressed as a bilinear term in the objective function. For a traditional bilinear optimization problem, iterative linear programming method can be applied to find the optimal solution(s). In the context of semidefinite programming, the optimization problem (30) can be tackled by iteratively solving the convex problem sequence (23) and (24).

The meaning of the direction matrix W can also provide us some intuition about the inner working of the convex iteration algorithm. Let's define matrix subspace \mathcal{S}_n as

$$\mathcal{S}_n \triangleq \{(I - W)X(I - W) | X \in S_+^N\} \quad (31)$$

It can be shown that the orthogonal compliment of \mathcal{S}_n is

$$\mathcal{S}_n^\perp = \{WXW | X \in S_+^N\} \quad (32)$$

The optimal solution to semidefinite program (23) X^* can be decomposed into two components (33). The first component is the projection of X^* onto subspace \mathcal{S}_n , which is $(I - W)X^*(I - W)$. The second component is the projection of X^* onto subspace \mathcal{S}_n^\perp , which is WX^*W .

$$X^* = (I - W)X^*(I - W) + WX^*W \quad (33)$$

According to Eckart-Young Theorem, the best rank-one approximation of X^* in terms of Frobenius norm distance is:

$$\hat{X}^* = U(:, 1)\Lambda(1, 1)U(:, 1)^T \quad (34)$$

It can be shown that the following equality holds:

$$(I - W)X^*(I - W) = U(:, 1)\Lambda(1, 1)U(:, 1)^T \quad (35)$$

Therefore, the projection of X^* onto \mathcal{S}_n is \hat{X}^* . Hence, polar direction $-W$ can be regarded as pointing toward the set of all rank-1 positive semidefinite matrices whose nullspace contains that of X^* .

D. Chordal Conversion

Coming back to Formulation 1 and first setting aside the rank constraint, a SDP programming problem needs to be solved. In most of the SDP solvers, the primal-dual interior-point method is adopted. The disadvantage of the primal-dual interior-point method is that it is time-consuming to construct the dense Schur complement matrix when solving large-scale problems. To address this drawback, the underlying aggregated sparsity of the power network is exploited by researchers [27], [33]. The semidefinite completion theory allows us to exploit the chordal sparsity of radial distribution networks [37]. The semidefinite completion theorem states that a symmetric matrix is positive semidefinite completable if and only if all of the small matrices associated with the maximal cliques of the graph derived from the whole matrix are positive semidefinite. This property allows the SDP problem to be converted into another form with smaller-sized positive semidefinite variables. The details of the conversion method are described in [26], [38]. When decomposing the graph of large networks, the intersections of maximal cliques are not empty. Thus, equality constraints of the intersection areas are introduced which may increase the dimension of the Schur complement matrix. Decisions need to be made to determine the trade-off between the sparsity and order of the Schur complement matrix. Some heuristic algorithms of clique amalgamation were developed in [26], [33].

By adopting chordal conversion, the original three-phase OPF problem (Formulation 1) can be reformulated as follows:

Formulation 3:

$$\min_X \sum_{l=1}^{N_A} C_l (X_l^{ext}) \quad (36)$$

subject to:

$$X_l^{ext} \in B^{(l)}, \quad l = 1, 2, \dots, N_A \quad (37)$$

$$X_l^{ext(r)} = X_r^{ext(l)}, \quad l, r = 1, 2, \dots, N_A \quad (38)$$

$$X_l^{ext} \succeq 0, \quad l = 1, 2, \dots, N_A \quad (39)$$

$$\text{rank}(X_l^{ext}) = 1, \quad l = 1, 2, \dots, N_A \quad (40)$$

where $B^{(l)}$ is the feasible region of X_l^{ext} satisfying

$$P_{G_k}^p - P_{D_k}^p = \text{Tr}\{\mathbf{Y}_k^p(l) X_l^{ext}\}, \quad k \in A_l$$

$$Q_{G_k}^p - Q_{D_k}^p = \text{Tr}\{\bar{\mathbf{Y}}_k^p(l) X_l^{ext}\}, \quad k \in A_l$$

$$\underline{P}_k - P_{D_k}^p \leq \text{Tr}\{\mathbf{Y}_k^p(l) X_l^{ext}\} \leq \bar{P}_k - P_{D_k}^p, \quad k \in A_l \setminus G$$

$$\underline{Q}_k - Q_{D_k}^p \leq \text{Tr}\{\bar{\mathbf{Y}}_k^p(l) X_l^{ext}\} \leq \bar{Q}_k - Q_{D_k}^p, \quad k \in A_l \setminus G$$

$$\text{Tr}\{\mathbf{Y}_{ik}^p(l) X_l^{ext}\}^2 + \text{Tr}\{\bar{\mathbf{Y}}_{ik}^p(l) X_l^{ext}\}^2 \leq (S_{ik}^{p \max})^2, \quad k \in A_l \cap G$$

$$(\underline{V}_k^p)^2 \leq \text{Tr}\{M_k^p(l) X\} \leq (\bar{V}_k^p)^2, \quad k \in A_l$$

A_l is the set of nodes in the l -th area. A_l^{ext} denotes the set of nodes in the l -th extended area which is defined as the union of A_l and the nodes of the other areas directly connected to the l -th area. A more detailed description of the extended area

concept is provided in [23]. V_l^{ext} denotes the voltage vector with the nodes in A_l^{ext} . $X_l^{ext(r)}$ is the sub-matrix of X_l^{ext} collecting the columns and rows of X_l^{ext} corresponding to the voltages of $A_l^{ext(r)} = \{A_l^{ext} \cap A_r^{ext}\}$.

The decomposition of rank constraint (21) is obvious. If matrix X is rank-one, then all the sub-matrices X_l^{ext} are rank-one. If all the sub-matrices X_l^{ext} are rank-one, then voltage vector V can be constructed with the results of singular value decomposition of all sub-matrices X_l^{ext} . Consequently, matrix X can be obtained from V .

E. Chordal Conversion Based Convex Iteration

By synergistically combining the chordal conversion method and the convex iteration technique, we propose a new iterative three-phase OPF solution algorithm as follows.

Formulation 4:

Step 1:

$$\min_X \sum_{l=1}^{N_A} C_l (X_l^{ext}) + \sum_{l=1}^{N_A} w_l \text{Tr}(X_l^{ext} W_l^*) \quad (41)$$

s.t.

$$X_l^{ext} \in B^{(l)}, \quad l = 1, 2, \dots, N_A \quad (42)$$

$$X_l^{ext(r)} = X_r^{ext(l)}, \quad l, r = 1, 2, \dots, N_A \quad (43)$$

$$X_l^{ext} \succeq 0, \quad l = 1, 2, \dots, N_A \quad (44)$$

Step 2:

$$W_l = U_j(:, 2 : N_{X_l^{ext}}) U_j(:, 2 : N_{X_l^{ext}})^T \quad (45)$$

where the size of X_l^{ext} is $N_{X_l^{ext}} \times N_{X_l^{ext}}$. U_j is obtained from the singular value decomposition.

$$X_j^{ext} = U_j \Lambda_j U_j^T \quad (46)$$

At a global optimum where the trace regularization term equals to zero, Formulation 4 becomes the convex equivalent of Formulation 3. The feasible set in Formulation 4 contains all rank-one symmetric matrices. An optimal rank-one solution X_{opt}^* from Formulation 4 will also minimize the objective function of Formulation 3.

The convergence to global optimality from an arbitrary initial point is not guaranteed. However, the algorithm will always arrive at a stalling point when the trace regularization term no longer decreases due to the monotonically non-increasing objective function sequence [36]. To re-start the algorithm with new search directions, the randomization technique can be leveraged [36]. Specifically with rank-one constraints, the direction matrices can be reinitialized as:

$$W_l = U_j(:, 2 : N_{X_l^{ext}}) (U_j(:, 2 : N_{X_l^{ext}})^T + \text{rand}(N_{X_l^{ext}}, 1) U_j(:, 1)^T)$$

However, the re-start process may fail by converging to another or the same stalling point with a rank larger than one. In addition, the re-start process could make the algorithm much more time-consuming.

F. Greedy Partition of the Grid

The computational efficiency of the chordal conversion based convex iteration algorithm depends heavily on the choice of grid partition scheme. This subsection develops a greedy algorithm to find an appropriate grid partition scheme. The algorithm development is motivated by the relationship between the computational complexity of the SDP problem in the first step of Formulation 4 and the nonzero elements in the search direction matrix.

A closer look is taken firstly at the computational efficiency of the interior point method which is adopted by most of the existing SDP solvers including SeDuMi [39], SDPA, and MOSEK. As SeDuMi is one of the most popular open source SDP solver package, it is chosen for illustration purpose in this subsection.

The SDP in Formulation 4 is first transformed to the standard conic form. The standard conic form of the SDP in formulation 4 can be written as follows.

$$\begin{aligned} \min & c^T x \\ & Ax = b \\ & x \in \mathcal{S}^+ \end{aligned}$$

where x is the vectorized primal variable and \mathcal{S}^+ is the semidefinite cone. In the primal-dual interior point method, scaling technique [40] is widely used. AHO [41], NT [42], and HKM [43] scaling are the most popular ones. With NT scaling adopted in SeDuMi, the scaling factor D [40], [44] is introduced to obtain the search direction in its iterative wide region method. Preconditioned gradient method is adopted in SeDuMi to obtain the inverse of ADA^T . In the preconditioning step, Cholesky decomposition of matrix ADA^T is performed. This is the most computationally expensive process in solving large-scale SDP problems. The computation cost of Cholesky decomposition heavily depends on the number of non-zero elements in matrix ADA^T . Therefore, to reduce the computation time, a greedy grid partition algorithm should search for the grid partition scheme which results in the least number of non-zero elements in matrix ADA^T .

For linear programming, the process of selecting the matrix ADA^T with the smallest number of non-zero elements can be accomplished by selecting matrix AA^T . This is because the sparsity patterns of the matrices ADA^T and AA^T are the same. Although this relationship doesn't hold for semidefinite programming, it still provides a good approximation. In other words, as long as the sparsity pattern does not vary a lot among different grid decomposition schemes, the partition scheme with smaller-sized AA^T matrix is more computationally efficient in general. Based on this approximation, a greedy algorithm is developed to find the partition scheme which yields a AA^T matrix with the smallest size. The greedy algorithm can be carried out as in algorithm 1.

IV. NUMERICAL STUDY

The proposed chordal based convex iteration algorithm with greedy grid partition scheme is implemented in YALMIP [45]. Simulations are conducted on the IEEE 4-bus, 10-bus, 13-bus, 34-bus, 37-bus, 123-bus, and 906-bus three-phase test

Algorithm 1 Greedy algorithm for grid partition

```

Initialize  $n_s = 1$ 
while 1 do
  if  $n_s = 0$  then
    break
  else
     $n_{temp} = n_s$ 
    for  $i = 1 : n_s$  do
      search for a possible cut in subarea  $i$ ;
      if there exists a cut which reduces the size of  $AA^T$ 
      then
        search along the edges in subarea  $i$ ; find the cut
        which reduces the size of  $AA^T$  the most,
         $n_{temp} = n_{temp} + 1$  and record the edge as a cut.
      else
        subarea  $i$  is finalized, i.e.
        no more search will be performed in subarea  $i$ ;
         $n_{temp} = n_{temp} - 1$ .
      end if
    end for
     $n_s = n_{temp}$ 
  end if
end while

```

feeders to validate 1) the optimality and feasibility of the solutions from the proposed convex iteration algorithm, 2) the computational efficiency of the greedy grid partition scheme, and 3) the scalability of the chordal conversion based convex iteration algorithm. A Dell workstation with a 64-bit Intel Xeon Quad Core CPU at 3.30 GHz with 16 GB of RAM is used to perform the simulations.

A. Solution Optimality and Feasibility

The IEEE three-phase test feeders are modified to account for scenarios where the supply offer prices on the three phases are different. In the IEEE 4-bus test feeder, the loads on three phases at node 4 are set as 1800KW, 1600KW, and 1400KW. The supply offer prices of the three phases are set as \$1/KWh, \$0.5/KWh, and \$0.2/KWh. Distribution generations are assumed to be located on node 4 with a generation capacity of 200KW per phase. In the 10-bus test feeder [23], the loads on the three phases are set as 700KW, 530KW, and 600KW to create unbalanced scenario. The supply offer prices of the three phases are set as \$1/KWh, \$0.3/KWh, and \$0.6/KWh. Distributed generations are placed on node 5 and 7 with a generation capacity of 50KW per node per phase. In the IEEE 13-bus test feeder, the load profile on the three phases is kept the same as 1175KW, 1039KW, and 1252KW. Distributed generations are placed on node 611, 652, 671, and 634 with a generation capacity of 50KW per node per phase. The supply offer prices of the three phases are set as \$0.6/KWh, \$0.3/KWh, and \$1/KWh. For the IEEE 34-bus test feeder, 50% load profile is adopted to avoid incorporating discrete control variables of the voltage regulators. The loads on the three phases are 303KW, 292KW, and 289.5KW. The distributed generations are placed on node 814, 836, and

890 with generation capacity of $20KW$ per node per phase. The supply offer prices of three phases are set as $\$1/KWh$, $\$0.9/KWh$, and $\$0.8/KWh$. For the IEEE 37-bus test feeder, the distributed generations are placed on node 701, 704, 707, 711, 744, 730, and 734 with generation capacity of $50KW$ per node per phase. The supply offer prices of three phases are set as $\$0.6/KWh$, $\$0.3/KWh$, and $\$1/KWh$. For the IEEE 123-bus test feeder, the distributed generations are placed on node 7, 18, 25, 35, 44, 54, 72, 76, 89, 97, and 105, with generation capacity of $50KW$ per node per phase. The supply offer prices of three phases are set as $\$1/KWh$, $\$0.3/KWh$, and $\$0.6/KWh$. For the IEEE European LV test feeder with 906 nodes, the distributed generations are placed on node 145, 155, 391, 707, and 745 with generation capacity of $0.5KW$ per node per phase. The supply offer prices of three phases are set as $\$0.6/KWh$, $\$0.7/KWh$, and $\$0.5/KWh$.

To illustrate the optimality and feasibility of solutions under the proposed algorithm, a comparison of the solutions obtained from traditional methods, including Powell method [46], [47] and interior-point method [48], [49], and the proposed convex iteration method is shown in Table I. Additional test scenarios are created by varying the supply offer prices of the DERs.

TABLE I
COMPARISON OF TRADITIONAL METHODS AND THE CONVEX ITERATION METHOD WITH DIFFERENT PRICES FOR DERs

Test system	Prices of three phases (\$/kWh)	Objective value (\$/hour)		
		Powell	Interior Point	Convex Iteration
4-bus test feeder	1/0.5/0.2	3121.9	3121.9	3121.9
	0.9/0.45/0.18	3091.9	3091.9	3086.9
10-bus test feeder	1/0.3/0.6	1229.2	1229.2	1229.1
	0.8/0.24/0.48	1191.4	1191.4	1191.3
13-bus test feeder	0.6/0.3/1	2345.4	2345.4	2345.4
	0.48/0.24/0.8	2290.2	2290.2	2290.2
34-bus test feeder	1/0.9/0.8	832.7	832.7	830.8
	0.9/0.81/0.72	816.5	816.5	815.4
37-bus test feeder	0.6/0.3/1	1740.3	1740.3	1739.5
	0.54/0.27/0.9	1675.9	1675.9	1675.4
123-bus test feeder	1/0.3/0.6	2414.6	2414.5	2413.6
	0.8/0.24/0.48	2205.6	2205.6	2205.0
906-bus test feeder	0.6/0.7/0.5	38.4	38.3	38.2
	0.54/0.63/0.45	37.9	37.9	37.7

As shown in Table I, the proposed convex iteration approach achieves lower objective values on 11 out of 14 test scenarios. The traditional methods arrive at the same solution as the proposed convex iteration method on the other 3 test scenarios. As the size of the test feeder increases, it becomes more difficult for the traditional methods to match the performance of the proposed convex iteration algorithm.

To illustrate the global optimality and feasibility of the proposed algorithm, another comparison of solutions derived from the SDP relaxation method [11], [13], [23] and the proposed convex iteration method with the default setting is shown in Table II.

It can be seen from Table II that the SDP relaxation method does not yield a rank-one solution by directly removing the rank constraint. For the IEEE 4-bus, 10-bus and 13-bus test feeders, the grids do not need to be partitioned. For the

TABLE II
COMPARISON OF THE SDP RELAXATION METHOD AND THE CONVEX ITERATION METHOD WITH DIFFERENT PRICES FOR THREE PHASES

Test system	Method	Rank of solution	Objective value (\$/hour)
4-bus test feeder	SDP relaxation	3	3085.6
	convex iteration	1	3121.9
10-bus test feeder	SDP relaxation	7	1216.3
	convex iteration	1	1229.1
13-bus test feeder	SDP relaxation	3	2319.5
	convex iteration	1	2345.4
34-bus test feeder	SDP relaxation	6*	831.8
	convex iteration	1	830.8
37-bus test feeder	SDP relaxation	1*	1739.5
	convex iteration	1	1739.5
123-bus test feeder	SDP relaxation	6*	2413.6
	convex iteration	1	2413.6
906-bus test feeder	SDP relaxation	6*	38.2
	convex iteration	1	38.2

IEEE 34-bus, 37-bus, 123-bus, and 906-bus test feeders, the same grid partition scheme is adopted for both the SDP relaxation and the proposed convex iteration methods. The star symbol, *, represents the highest rank among all partitioned areas. The SDP relaxation method only succeeds in finding a feasible rank-one solution for the 37-bus test feeder. The high rank solutions in other cases do not have any physical meaning. In most cases, the solution of the SDP relaxation method provides a lower bound of the original non-convex optimization problem. For the 34-bus test feeder, the SDP solver stops at a near-global optimal solution of the relaxed problem, which has a higher value than that of the convex iteration method. The numerical difficulty is caused by the extremely long and short distribution lines [50]. On the other hand, the proposed chordal conversion based convex iteration algorithm always produces a rank-1 solution, which is the global optimum.

TABLE III
COMPARISON OF THE SDP RELAXATION METHOD AND THE CONVEX ITERATION METHOD WITH SAME PRICES FOR THREE PHASES

Test system	Method	Rank of solution	Power loss (kW)
4-bus test feeder	SDP relaxation	1	325.9
	convex iteration	1	325.9
10-bus test feeder	SDP relaxation	1	12.2
	convex iteration	1	12.2
13-bus test feeder	SDP relaxation	1	89.4
	convex iteration	1	89.4
34-bus test feeder	SDP relaxation	6*	38.3
	convex iteration	1	37.5
37-bus test feeder	SDP relaxation	1	26.4
	convex iteration	1	26.4
123-bus test feeder	SDP relaxation	6*	32
	convex iteration	1	34.7
906-bus test feeder	SDP relaxation	7*	1.5
	convex iteration	1	1.3

If the prices are set to be $\$1/KWh$ for all three phases, the original problem is equivalent to minimization of the total power losses. As shown in Table III, the SDP relaxation method is able to find the global optimum for the three small-scaled systems, which is consistent with the analysis in section III.A and reference [23].

At last, a comprehensive comparison between the penalized SDP method [18] and the proposed convex iteration algorithm is conducted. The comparison results are shown in Table IV.

TABLE IV
COMPARISON OF THE PENALIZED SDP METHOD AND THE CONVEX ITERATION METHOD

Test system	Method	$\text{eig}^2/\text{eig}^1$	Power injection error (kW)
4-bus test feeder	penalized SDP	9.1×10^{-9}	5.6×10^{-3}
	convex iteration	2.6×10^{-9}	3.9×10^{-3}
10-bus test feeder	penalized SDP	7.7×10^{-7}	5.2×10^{-3}
	convex iteration	2.2×10^{-9}	6.8×10^{-3}
13-bus test feeder	penalized SDP	3.8×10^{-7}	0.2208
	convex iteration	3.2×10^{-9}	0.0629
34-bus test feeder	penalized SDP	1.2×10^{-5}	3.24
	convex iteration	6.0×10^{-8}	2.41
37-bus test feeder	penalized SDP	3.0×10^{-6}	1.54
	convex iteration	3.0×10^{-6}	1.54
123-bus test feeder	penalized SDP	2.8×10^{-5}	13.21
	convex iteration	1.2×10^{-8}	1.21
906-bus test feeder	penalized SDP	5.1×10^{-5}	6.7
	convex iteration	6.0×10^{-8}	2.3

For the IEEE 4-bus, 10-bus, and 13-bus test feeders, the comparison is performed without graph partition. Although the penalized SDP method did obtain a rank-one solution, the ratio of the second largest eigenvalue of matrix X to its largest eigenvalue is much larger than that of the proposed convex iteration method. Moreover, as shown in Table IV, the power injection error obtained from SVD of the rank-one solution of the penalized SDP method is much larger than that of the proposed convex iteration method.

For the IEEE 34-bus, 37-bus, 123-bus, and 906-bus test feeders, the comparison is performed with the same graph partition scheme obtained from the greedy algorithm. For IEEE 34-bus, 123-bus, and 906-bus test feeders, the penalized SDP method fails to find a rank-one solution. In IEEE 123-bus, one of the partitioned areas containing nodes 44, 47, 48, 49, and 50 is selected for verification. Under the penalized SDP method, the non-negligible eigenvalues of the variable matrix are 15.8738, 0.0004, 0.0004, 0.0002, 0.0002, and 0.0001. The p.u. complex voltage of the boundary node 50 obtained from rank-one approximation are different. The complex voltage of the boundary point under the penalized SDP method are $[1.0167 - 0.0283j, -0.5260 - 0.8964j, -0.5035 + 0.8964j]$ and $[1.0170 - 0.0280j, -0.5262 - 0.8969j, -0.5044 + 0.8967j]$ in two different extended areas. The power injection error under the penalized SDP method is also much larger than that of the proposed convex iteration method.

TABLE V
COMPUTATION TIME OF IEEE 4-BUS TEST FEEDER

Number of partition areas	Computation time (s)	Number of iterations	Number of Nonzero Elements
1	0.346	4	3.92×10^4
2	0.373	4	2.95×10^4
*2	0.373	4	2.95×10^4
3	0.484	4	3.63×10^4
4	0.577	4	4.25×10^4

TABLE VI
COMPUTATION TIME OF IEEE 13-BUS TEST FEEDER

Number of partition areas	Computation time (s)	Number of iterations	Number of Nonzero Elements
1	68.397	20	2.12×10^6
2	10.789	14	5.39×10^5
3	9.659	15	4.22×10^5
*4	8.714	16	3.61×10^5
4	7.732	16	3.18×10^5
5	6.567	13	3.24×10^5
6	6.602	14	2.77×10^5
7	5.768	14	2.27×10^5
8	6.020	14	2.27×10^5
9	6.374	15	2.27×10^5
13	8.019	16	2.53×10^5

B. Effectiveness of the Greedy Grid Partition Scheme

To validate the effectiveness of the proposed greedy grid partition scheme, simulations are conducted on the IEEE 4-bus and 13-bus test feeders under all possible grid partition scenarios. An exhaustive search for all possible partition scenarios is conducted. The computation times of all scenarios are recorded. The results are then grouped by the number of partitioned areas. The computation times being reported in Table V and VI are the shortest computation times for each number of partition areas using MOSEK. The computation times obtained from the greedy partition scheme is denoted by *.

It can be seen from Table IV and V that the computation time of the proposed algorithm is approximately proportional to the number of nonzero elements in matrix ADA^T . The greedy algorithm successfully found grid partitioning schemes with very reasonable computation times. In the IEEE 4-bus test feeder, the computation time with the greedy partition scheme is almost the same as the shortest computation time found by exhaustive search. In the IEEE 13-bus test feeder, the computation time with the greedy partition scheme is only 3 seconds longer than the shortest computation time.

C. Scalability of the Proposed Algorithm

As shown in Table VII, the computation times of the three-phase OPF problems on all seven IEEE test feeders is within 2 minutes using the entry level Dell workstation. The combination of the chordal based conversion technique and the greedy grid partition scheme made the proposed algorithm computationally efficient.

TABLE VII
SCALABILITY OF PROPOSED ALGORITHM

Test system	Computation time (s)	Number of iterations	Number of Nonzero Elements	Rank of Solution
4-bus	0.373	4	2.95×10^4	1
10-bus	12.127	29	2.53×10^5	1
13-bus	8.714	16	3.61×10^5	1
34-bus	4.161	3	1.25×10^6	1
37-bus	3.261	1	2.06×10^6	1
123-bus	27.182	3	4.93×10^6	1
906-bus	79.799	3	1.32×10^7	1

V. CONCLUSION

This paper develops a chordal conversion based convex iteration algorithm to solve the three-phase OPF problem. A greedy grid partition scheme is also developed to improve the computational efficiency of the proposed algorithm. The simulation results show that the greedy algorithm can find an appropriate grid partition scheme which has similar computation time to that of the best partition found from the exhaustive search. At last, the scalability of the proposed algorithm is validated through simulations on the IEEE 123-bus and 906-bus test feeders. The proposed OPF algorithm can find the global optimal solutions within 2 minutes on an entry level Dell workstation. However, it should be noted that it is possible for the proposed convex iteration approach to converge to a local optimum and the re-start strategy may fail. Therefore, the proposed convex iteration algorithm does not guarantee convergence to global optimum solution(s) in all distribution feeders.

REFERENCES

- [1] M. Liu, S. K. Tso, and Y. Cheng, "An extended nonlinear primal-dual interior-point algorithm for reactive-power optimization of large-scale power systems with discrete control variables," *IEEE Trans. Power Syst.*, vol. 17, no. 4, pp. 982–991, Nov 2002.
- [2] M. B. Liu, C. A. Canizares, and W. Huang, "Reactive power and voltage control in distribution systems with limited switching operations," *IEEE Trans. Power Syst.*, vol. 24, no. 2, pp. 889–899, May 2009.
- [3] Y. P. Agalgaonkar, B. C. Pal, and R. A. Jabr, "Distribution voltage control considering the impact of PV generation on tap changers and autonomous regulators," *IEEE Trans. Power Syst.*, vol. 29, no. 1, pp. 182–192, Jan 2014.
- [4] D. Ranamuka, A. P. Agalgaonkar, and K. M. Muttaqi, "Online coordinated voltage control in distribution systems subjected to structural changes and DG availability," *IEEE Trans. Smart Grid*, vol. 7, no. 2, pp. 580–591, March 2016.
- [5] H. W. Dommel and W. F. Tinney, "Optimal power flow solutions," *IEEE Trans. Power App. Syst.*, vol. PAS-87, no. 10, pp. 1866–1876, Oct. 1968.
- [6] O. Alsac and B. Stott, "Optimal load flow with steady-state security," *IEEE Trans. Power App. Syst.*, vol. PAS-93, no. 3, pp. 745–751, May 1974.

- [7] G. C. Contaxis, C. Delkis, and G. Korres, "Decoupled optimal load flow using linear and quadratic programming," *IEEE Trans. Power Syst.*, vol. 1, no. 2, pp. 1–7, May 1986.
- [8] B. Ghaddar, J. Marecek, and M. Mevissen, "Optimal power flow as a polynomial optimization problem," *IEEE Trans. Power Syst.*, vol. 31, no. 1, pp. 539–546, Jan. 2016.
- [9] I. M. Nejdawi, K. A. Clements, and P. W. Davis, "An efficient interior-point method for sequential quadratic programming based optimal power flow," *IEEE Trans. Power Syst.*, vol. 15, no. 4, pp. 1179–1183, Nov. 2000.
- [10] P. E. O. Yumbla, J. M. Ramirez, and C. A. C. Coello, "Optimal power flow subject to security constraints solved with a particle swarm optimizer," *IEEE Trans. Power Syst.*, vol. 23, no. 1, pp. 33–40, Feb. 2008.
- [11] X. Bai, H. Wei, K. Fujisawa, and Y. Wang, "Semidefinite programming for optimal power flow problems," *Int. J. Elect. Power Energy Syst.*, vol. 30, no. 6, pp. 383–392, Sep. 2008.
- [12] J. Lavaei, D. Tse, and B. Zhang, "Geometry of power flows in tree networks," in *Proc. 2012 IEEE Power & Energy Soc. General Meeting*, Jul. 2012, pp. 1–8.
- [13] J. Lavaei and S. H. Low, "Zero duality gap in optimal power flow problem," *IEEE Trans. Power Syst.*, vol. 27, no. 1, pp. 92–107, Feb. 2012.
- [14] S. H. Low, "Convex relaxation of optimal power flow-part II: Exactness," *IEEE Trans. Control Netw. Syst.*, vol. 1, no. 2, pp. 177–189, June 2014.
- [15] L. Gan, N. Li, U. Topcu, and S. H. Low, "Exact convex relaxation of optimal power flow in radial networks," *IEEE Trans. Autom. Control*, vol. 60, no. 1, pp. 72–87, Jan. 2015.
- [16] S. You and Q. Peng, "A non-convex alternating direction method of multipliers heuristic for optimal power flow," in *Smart Grid Communications, 2014 IEEE Int. Conf. on*, Nov. 2014, pp. 788–793.
- [17] D. K. Molzahn, C. Jozs, I. A. Hiskens, and P. Panciatici, "A Laplacian-based approach for finding near globally optimal solutions to OPF problems," *IEEE Trans. Power Syst.*, vol. PP, no. 99, pp. 1–1, Apr. 2016.
- [18] R. Madani, S. Sojoudi, and J. Lavaei, "Convex relaxation for optimal power flow problem: Mesh networks," *IEEE Trans. Power Syst.*, vol. 30, no. 1, pp. 199–211, Jan 2015.
- [19] A. Y. S. Lam, B. Zhang, and D. N. Tse, "Distributed algorithms for optimal power flow problem," in *2012 51st IEEE Conf. on Decision and Control*, Dec. 2012, pp. 430–437.
- [20] B. H. Kim and R. Baldick, "A comparison of distributed optimal power flow algorithms," *IEEE Trans. Power Syst.*, vol. 15, no. 2, pp. 599–604, May 2000.
- [21] T. Erseghe, "Distributed optimal power flow using ADMM," *IEEE Trans. Power Syst.*, vol. 29, no. 5, pp. 2370–2380, Sep. 2014.
- [22] S. Magnusson, P. C. Weeraddana, and C. Fischione, "A distributed approach for the optimal power flow problem based on ADMM and sequential convex approximations," *IEEE Trans. Control Netw. Syst.*, vol. 2, no. 3, pp. 238–253, Sep. 2015.
- [23] E. Dall'Anese, H. Zhu, and G. B. Giannakis, "Distributed optimal power flow for smart microgrids," *IEEE Trans. Smart Grid*, vol. 4, no. 3, pp. 1464–1475, Sep. 2013.
- [24] S. Boyd, N. Parikh, E. Chu, B. Peleato, and J. Eckstein, "Distributed optimization and statistical learning via the alternating direction method of multipliers," *Foundations and Trends in Machine Learning*, vol. 3, no. 1, pp. 1–122, Jan. 2011.
- [25] A. Kalbat and J. Lavaei, "A fast distributed algorithm for decomposable semidefinite programs," in *2015 54th IEEE Conf. on Decision and Control*, Dec 2015, pp. 1742–1749.
- [26] M. S. Andersen, A. Hansson, and L. Vandenberghe, "Reduced-complexity semidefinite relaxations of optimal power flow problems," *IEEE Trans. Power Syst.*, vol. 29, no. 4, pp. 1855–1863, Jul. 2014.
- [27] R. A. Jabr, "Exploiting sparsity in SDP relaxations of the OPF problem," *IEEE Trans. Power Syst.*, vol. 27, no. 2, pp. 1138–1139, May 2012.
- [28] S. Bose, S. H. Low, T. Teeraratkul, and B. Hassibi, "Equivalent relaxations of optimal power flow," *IEEE Transactions Autom. Control*, vol. 60, no. 3, pp. 729–742, March 2015.
- [29] S. H. Low, "Convex relaxation of optimal power flow-part I: Formulations and equivalence," *IEEE Trans. Control Netw. Syst.*, vol. 1, no. 1, pp. 15–27, March 2014.
- [30] S. Kim, M. Kojima, M. Mevissen, and M. Yamashita, "Exploiting sparsity in linear and nonlinear matrix inequalities via positive semidefinite matrix completion," *Mathematical Programming*, vol. 129, no. 1, pp. 33–68, 2011.
- [31] X. Bai and H. Wei, "A semidefinite programming method with graph partitioning technique for optimal power flow problems," *Int. J. Elect. Power Energy Syst.*, vol. 33, no. 7, pp. 1309 – 1314, 2011.

- [32] M. Fukuda, M. Kojima, K. Murota, and K. Nakata, "Exploiting sparsity in semidefinite programming via matrix completion I: General framework," *SIAM J. Optimiz.*, vol. 11, no. 3, pp. 647–674, 2001.
- [33] D. K. Molzahn, J. T. Holzer, B. C. Lesieutre, and C. L. DeMarco, "Implementation of a large-scale optimal power flow solver based on semidefinite programming," *IEEE Trans. Power Syst.*, vol. 28, no. 4, pp. 3987–3998, Nov. 2013.
- [34] S. Bruno, S. Lamonaca, G. Rotondo, U. Stecchi, and M. L. Scala, "Unbalanced three-phase optimal power flow for smart grids," *IEEE Trans. Ind. Electron.*, vol. 58, no. 10, pp. 4504–4513, Oct. 2011.
- [35] B. Moradzadeh and K. Tomsovic, "Two-stage residential energy management considering network operational constraints," *IEEE Trans. Smart Grid*, vol. 4, no. 4, pp. 2339–2346, Dec. 2013.
- [36] J. Dattorro, *Convex Optimization and Euclidean Distance Geometry*. CA: Meboo Publishing, 2005.
- [37] R. Grone, C. R. Johnson, E. M. S, and H. Wolkowicz, "Positive definite completions of partial hermitian matrices," *Linear Algebra and its Applications*, vol. 58, pp. 109–124, 1984.
- [38] L. Vandenberghe and M. S. Andersen, "Chordal graphs and semidefinite optimization," *Foundations and Trends in Optimization*, vol. 1, no. 4, pp. 241–433, 2015.
- [39] J. Sturm, "Using SeDuMi 1.02, a MATLAB toolbox for optimization over symmetric cones," *Optimiz. Meth. Soft.*, vol. 11, no. 1, pp. 625–653, 1999.
- [40] ———, "Implementation of interior-point methods for mixed semidefinite and second order cone optimization problems," *Optimiz. Meth. Soft.*, vol. 17, no. 6, pp. 1105–1154, 2002.
- [41] F. Alizadeh, J. Haeberly, and M. Overton, "A new primal-dual interior-point method for semidefinite programming," in *Proc. 5th SIAM Conf. on Applied Linear Algebra*, Philadelphia, 1994, pp. 113–117.
- [42] Y. Nesterov and M. Todd, "Self-scaled barriers and interior-point methods for convex programming," *Mathematics of Operations Research*, vol. 22, no. 1, pp. 1–42, 1997.
- [43] C. Helmberg, F. Rendl, R. Vanderbei, and H. Wolkowicz, "An interior-point method for semidefinite programming," *SIAM J. Optimiz.*, vol. 6, pp. 342–361, 1996.
- [44] J. Sturm, "Primal-dual interior-point approach to semidefinite programming," Ph.D. dissertation, Tinbergen Institute of the Erasmus University, Rotterdam, The Netherlands, 1997.
- [45] J. Lofberg, "YALMIP : a toolbox for modeling and optimization in MATLAB," Sep. 2004, pp. 284–289.
- [46] A. M. Sasson, F. Vilorio, and F. Aboites, "Optimal load flow solution using the hessian matrix," *IEEE Trans. on Power App. Syst.*, vol. PAS-92, no. 1, pp. 31–41, Jan 1973.
- [47] S. N. Talukdar, T. C. Giras, and V. K. Kalyan, "Decompositions for optimal power flows," *IEEE Trans. on Power App. Syst.*, vol. PAS-102, no. 12, pp. 3877–3884, Dec 1983.
- [48] S. Granville, "Optimal reactive dispatch through interior point methods," *IEEE Trans. on Power Syst.*, vol. 9, no. 1, pp. 136–146, Feb 1994.
- [49] H. Wei, H. Sasaki, J. Kubokawa, and R. Yokoyama, "An interior point nonlinear programming for optimal power flow problems with a novel data structure," *IEEE Trans. on Power Syst.*, vol. 13, no. 3, pp. 870–877, Aug 1998.
- [50] W. H. Kersting, "Radial distribution test feeders," in *2001 IEEE Power Engineering Society Winter Meeting.*, vol. 2, Jan 2001, pp. 908–912 vol.2.